

## LABORATORY INVESTIGATIONS

Anesthesiology

1998; 88:984-92

© 1998 American Society of Anesthesiologists, Inc.

Lippincott-Raven Publishers

# Regional Cerebral Plasma Volume Response to Carbon Dioxide Using Magnetic Resonance Imaging

Jean-François Payen, M.D., Ph.D.,\* Albert Vâth, Ph.D.,† Blanche Koenigsberg,† Virginie Bourlier,† Michel Decorps, Ph.D.‡

**Background:** Noninvasive techniques used to determine the changes in cerebral blood volume in response to carbon dioxide are hampered by their limited spatial or temporal resolution or both. Using steady state contrast-enhanced magnetic resonance imaging, the authors determined regional changes in cerebral plasma volume (CPV) induced by hypercapnia in halothane-anesthetized rats.

**Methods:** Cerebral plasma volume was determined during normocapnia, hypercapnia and recovery in the dorsoparietal neocortex and striatum of each hemisphere, in cerebellum, and in extracerebral tissue of rats with either intact carotid arteries (group 1) or unilateral common carotid ligation (group 2). Another group was studied without injection of a contrast agent (group 3).

**Results:** Hypercapnia (partial pressure of carbon dioxide in arterial blood  $[Pa_{CO_2}] \approx 65$  mmHg) resulted in a significant increase in CPV in the striatum ( $+42 \pm 8\%$ ), neocortex ( $+34 \pm 6\%$ ), and cerebellum ( $+49 \pm 12\%$ ) compared with normocapnic CPV values (group 1). Carotid ligation (group 2) led to a marked reduction of the CPV response to hypercapnia in the ipsilateral striatum ( $+23 \pm 14\%$ ) and neocortex ( $+27 \pm 17\%$ ) compared with the unclamped side ( $+34 \pm 15\%$  and  $+38 \pm 16\%$ , respectively). No significant changes in CPV were found in extracerebral tissue. In both groups, the CPV changes were reversed by the carbon dioxide washout period. Negligible

changes in contrast imaging were detected during hypercapnia without administration of the contrast agent (group 3).

**Conclusions:** The contrast-enhanced magnetic resonance imaging technique is sensitive to detect noninvasively regional CPV changes induced by hypercapnia in rat brain. This could be of clinical interest for determining the cerebrovascular reactivity among different brain regions. (Key words: Contrast agent; hypercapnia; regional cerebral plasma volume.)

THE determination of cerebrovascular reactivity is clinically important, such as after head injury, subarachnoid hemorrhage, and in patients with carotid disease. The response of blood vessels to carbon dioxide or acetazolamide is usually quantified by measuring cerebral blood flow (CBF)<sup>1</sup> or CBF velocity.<sup>2</sup> Few data exist about cerebral blood volume (CBV) changes in response to carbon dioxide in humans, although experimental data show that CBF and CBV do not change in parallel.<sup>3-6</sup> Studies in humans have used single-photon emission computed tomography (SPECT), with <sup>99m</sup>Technetium as a marker for erythrocytes<sup>7,8</sup> and for human serum albumin.<sup>8</sup> These techniques are hampered, however, by limited spatial or temporal resolution, or both, and by the need for patient exposure to ionizing radiation. Because CBV differs greatly among brain regions,<sup>9,10</sup> a noninvasive determination of the regional CBV changes in response to carbon dioxide is required.

Contrast-enhanced magnetic resonance imaging (MRI) has been proposed as a tool to determine relative regional CBV<sup>11</sup> via two main approaches: first-pass imaging after injection of a bolus of a nondiffusible paramagnetic contrast agent (dynamic susceptibility-contrast MRI) or steady state imaging before and after administration of a nondiffusible paramagnetic or superparamagnetic long-lived contrast agent (steady state susceptibility-contrast MRI). In both methods, the intravascular compartmentalization of the contrast agent induces a difference in magnetic susceptibility ( $\Delta\chi$ ) between vascular and extravascular compartments. This susceptibility difference results in magnetic field perturbations that increase the decay rate ( $R_2^*$ ) of the

This article is accompanied by an Editorial View. Please see: Litt L: Sensitive physiological imaging with contrast-enhanced magnetic resonance imaging. ANESTHESIOLOGY 1998; 88:847-50.

\* Professor of Anesthesia.

† Research Assistant of INSERM.

‡ Director of INSERM 438 Unit.

Received from INSERM U438, Hôpital Albert Michallon, Grenoble, France. Submitted for publication July 25, 1997. Accepted for publication December 16, 1997. Supported by a grant from the the DAAD/HSP II program, Rhône-Alpes Region and the Fondation pour la Recherche Médicale. AMI-227 was provided by Guerbet Laboratories.

Address reprint requests to Dr. Payen: INSERM U438, Pavillon B, Hôpital A. Michallon, BP 217, CHU Grenoble, 38043 Grenoble Cedex 09 France. Address electronic mail to: jean-francois.payen@inserm-u438.ujf-grenoble.fr



## CO<sub>2</sub>-INDUCED REGIONAL CHANGES IN CEREBRAL PLASMA VOLUME

nuclear magnetic resonance (NMR) of tissue protons, resulting in an increase in the water peak line width. This effect is commonly called the susceptibility-induced  $T_2^*$  shortening ( $T_2^* = 1/R_2^*$ ) (see the appendix for more details). It has been shown that the local variation of the transverse relaxation rate induced by the contrast agent ( $\Delta R_2^*$ ) is linearly proportional to CBV,<sup>12,13</sup> assuming a constant plasma concentration of the contrast agent. Thus the determination of absolute CBV values requires the measurement of the proportionality constant. If the regional NMR signal intensity changes induced by perturbations in the partial pressure of carbon dioxide in arterial blood ( $P_{aCO_2}$ ) are converted to changes in  $\Delta R_2^*$ , the relative CBV changes in response to carbon dioxide can be monitored within different brain regions. However, because the contrast agent is a plasma marker, this method is sensitized to the measurement of cerebral plasma volume (CPV), where  $CBV = CPV + \text{cerebral erythrocyte volume}$ . No extrapolation to CBV should be made from one single-tracer method because of uncertainties about the precise value of the cerebral hematocrit value during carbon dioxide perturbations.<sup>5,6,8</sup>

The aim of the present study was to evaluate the feasibility and sensitivity of the steady state contrast-enhanced MRI technique during reversible moderate hypercapnia in anesthetized rats. The changes in relative CPV were measured in the dorsoparietal neocortex and the striatum of each hemisphere and in the cerebellum in two series of experiments: with intact carotid arteries, and with unilateral common carotid ligation, which produces asymmetrical CBF response to hypercapnia.<sup>14</sup> In addition, we investigated the effect of hypercapnia on the NMR signal intensity in the absence of contrast agent.

## Materials and Methods

### Animal Preparation

All experiments were approved by the National Animal Care and Use Committee. Fed Sprague-Dawley female rats (weight, 250–270 g) were studied. Anesthesia was induced with 4% halothane and then maintained with 1–1.5% halothane during surgery. One percent lidocaine was injected subcutaneously for local anesthesia at all surgical sites. After tracheostomy, the rats were mechanically ventilated with 0.5% halothane and 65% nitrous oxide–35% oxygen using the a rodent ventilator (model 804; Edco/NEMI, Medway, MA). Ventilation was

adjusted to maintain  $P_{aCO_2}$  at 30–35 mmHg. The fractional inspired oxygen concentration was continuously monitored (MiniOX I analyzer; Catalyst Research Corp., Owings Mills, MD). Normal saline containing pancuronium bromide (0.04 mg/ml) was infused intraperitoneally at a rate of 1–2 ml/h throughout the study. Rectal temperature was maintained at  $37 \pm 0.5^\circ\text{C}$  by a heated pad placed on the abdomen.

Three groups of rats were prepared. In group 1 ( $n = 7$  rats), a 0.7-mm indwelling catheter was inserted into the tail artery to monitor mean arterial blood pressure *via* a graphic recorder (8000S; Gould Electronics, Balmainvilliers, France). Blood gases ( $P_{aO_2}$ ,  $P_{aCO_2}$ ), arterial pH, and arterial hemoglobin concentration were measured from arterial blood samples  $<0.1$  ml (Radiometer ABL 510, Copenhagen, Denmark). Blood gases and arterial pH were corrected for rectal temperature. Another 0.7-mm catheter was inserted into the left femoral vein to inject the contrast agent. Group 2 ( $n = 7$  rats) and group 3 ( $n = 5$  rats) were prepared as group 1 was, except that the left common carotid artery was ligated. Mean arterial blood pressure and blood gases were monitored *via* a 0.7-mm catheter inserted into the carotid artery for these groups.

### Magnetic Resonance Imaging Experiments

Magnetic resonance imaging was performed with a Bruker MSL console (Bruker Spectrospin, Wissembourg, France) equipped with a 2.35-T, 40-cm diameter horizontal bore magnet and a 10-cm diameter home-built gradient system. The anesthetized rats were ventrally positioned in a specially designed stereotaxic device, including ear bars that secured the rat's skull. A 30-mm diameter surface coil was positioned directly above the brain. The animal was placed so that the bregma was located 5 mm above and 5 mm in front of the isocenter of the magnet. Good positioning was assessed by acquiring a  $T_1$ -weighted transverse scout image. After radiofrequency coil matching and tuning, the magnetic field homogeneity was adjusted to obtain a line width for water smaller than 0.5 ppm in the whole brain. Two coronal slices (2 mm and 5 mm below the bregma) were chosen from the scout image. Eight images of both slices were obtained using a multiple-gradient-echo sequence with an interecho spacing of 6 ms (repetition time  $T_R = 1.5$  s; slice thickness = 1 mm; field of view = 4 cm;  $64 \times 64$  image matrix; number of averages = 2; number of echoes = 8; echo times = 6, 12, 18, 24, 30, 36, 42, 48 ms). A single-phase encoding



gradient was applied at each excitation. Acquisition of images lasted about 3 min.

To induce susceptibility effects, a solution of an iron dextran-coated, ultra-small (particles that were 30 nm in diameter), superparamagnetic iron oxide agent (AMI-227 [Sinerem]; Guerbet, Aulnay-sous-Bois, France) was injected *via* the femoral vein in group 1 and group 2 animals at a dose of 200  $\mu\text{mol}$  iron per kilogram body mass. At this dose, the plasma elimination half-time of the contrast agent is 4.5 h (Guerbet Laboratory; unpublished data). No contrast agent was administered to group 3.

#### Experimental Protocol

Animals were subjected to successive periods of normocapnia, hypercapnia, and recovery (carbon dioxide washout). Each  $\text{Pa}_{\text{CO}_2}$  period lasted about 20 min, including the determination of mean arterial blood pressure, blood gases, and arterial pH, and the acquisition of the NMR images. If the initial arterial pH was  $<7.25$ , or the initial  $\text{Pa}_{\text{O}_2}$  was  $<100$  mmHg, the animal was excluded from the study. The control period was normocapnia ( $\text{Pa}_{\text{CO}_2} \approx 35$  mmHg), during which pre- and postcontrast (5-min after the injection of contrast agent) images were acquired. Hypercapnia was then induced by adding 6% carbon dioxide to the initial breathing mixture ( $\text{Pa}_{\text{CO}_2} \approx 65$  mmHg). Nuclear magnetic resonance images were collected after 15-min exposure to hypercapnia. Normocapnia was then restored (recovery), and all the measurements were carried on again after a 15-min period of equilibrium. When the cycle of measurements was ended, the animals were killed by administration of 5% halothane in pure nitrous oxide.

#### Data Analysis

Image postprocessing and determination of the changes in relative CPV were performed using an Axil320 desktop work station (Axil Computer Inc., Santa Clara, CA). For each  $\text{Pa}_{\text{CO}_2}$  period,  $T_2^*$  images were obtained by least-square fitting of the intensity data at each echo time to a monoexponential function on a pixel-by-pixel basis. Differences in relaxation rates in each pixel were then calculated according to the formula:

$$\Delta R_2^* = \frac{1}{T_{2^*}^{\text{post}}} - \frac{1}{T_{2^*}^{\text{pre}}} \quad (1)$$

with  $T_{2^*}^{\text{pre}}$  and  $T_{2^*}^{\text{post}}$  being the decay time constants before and after administration of the contrast agent.

The  $\Delta R_2^*$  values were obtained from the  $T_2^*$  postcontrast values during normocapnia, hypercapnia, and recovery, which allowed  $\Delta R_2^*$  maps to be obtained. The regions of interest were the dorsoparietal neocortex and the striatum of the two hemispheres, and the cerebellum. The selection of cerebral regions was made from the superficial slice (for the neocortex) and deep slice (for the striatum and the cerebellum) by comparing the data to that of an atlas of anatomy.<sup>15</sup> In addition,  $\Delta R_2^*$  values in extracerebral tissue were determined. Large  $\Delta R_2^*$  values ( $>120 \text{ s}^{-1}$ ) corresponding probably to large vessels (radius  $>80 \mu\text{m}$ ) were discarded. A correction for plasma clearance of the contrast agent was applied because the postcontrast experiments lasted approximately 60 min. The plasma concentration of the contrast agent was assumed to decay exponentially over the time, according to the formula:

$$C(t) = C_0 \exp^{-\lambda t} \quad (2)$$

where  $t$  is the time after administration of the contrast agent and  $\lambda$  is the elimination time constant of the contrast agent ( $= 0.154 \text{ h}^{-1}$  at 200  $\mu\text{mol}$  iron per kilogram of body mass). Because  $\Delta R_2^*$  depends linearly on both plasma concentration of the contrast agent and CPV:

$$\Delta R_2^*(t) \propto C(t) \text{CPV} \quad (3)$$

the corrected  $\Delta R_2^*$  value ( $\Delta R_{2^*}^{\text{cor}}$ ) was obtained from the measured  $\Delta R_2^*$  value ( $\Delta R_{2^*}^{\text{mes}}$ ) at each time point using the equation:

$$\Delta R_{2^*}^{\text{cor}} = \Delta R_{2^*}^{\text{mes}} \exp^{\lambda t} \quad (4)$$

No contrast agent was given to group 3. The  $\Delta R_2^*$  values were calculated as the  $1/T_2^*$  changes observed in cerebral and extracerebral regions from normocapnia to hypercapnia.

#### Statistical Analysis

Data were expressed as means  $\pm$  SD. Analysis for statistical significance was performed within each group of rats using one-way analysis of variance for repeated measurements (StatView SE program; Abacus Concepts, Berkeley, CA). Each value was compared with that obtained at the control period (normocapnia) using the Scheffé F test. The differences between the two hemispheres (striatum, neocortex) or between the two groups of rats were tested using a paired or an unpaired Student's  $t$  test, respectively. Significance was declared when  $P < 0.05$ .



CO<sub>2</sub>-INDUCED REGIONAL CHANGES IN CEREBRAL PLASMA VOLUME**Table 1. Physiological and Biochemical Data in Group 1 (No Carotid Occlusion) and in Group 2 (Left Carotid Occlusion) throughout the Successive Pa<sub>CO<sub>2</sub></sub> Periods**

	Normocapnia	Hypercapnia	Recovery
MABP (mmHg)			
Group 1	107 ± 13	104 ± 18	110 ± 14
Group 2	108 ± 10	107 ± 15	114 ± 13
Temperature (°C)			
Group 1	36.7 ± 0.7	36.7 ± 0.8	36.6 ± 0.6
Group 2	37.2 ± 0.3	37.3 ± 0.4	37.2 ± 0.4*
PaO <sub>2</sub> (mmHg)			
Group 1	164 ± 13	157 ± 14	152 ± 19
Group 2	128 ± 13†	130 ± 7†	125 ± 11†
PaCO <sub>2</sub> (mmHg)			
Group 1	35.8 ± 2.0	68.2 ± 10.1	37.2 ± 4.1
Group 2	35.2 ± 3.5	67.5 ± 8.2	37.3 ± 3.4
Arterial pH			
Group 1	7.42 ± 0.04	7.19 ± 0.04	7.40 ± 0.04
Group 2	7.40 ± 0.04	7.18 ± 0.03	7.37 ± 0.03
Hemoglobin (g · L <sup>-1</sup> )			
Group 1	13.1 ± 0.9	12.6 ± 1.0	12.5 ± 1.0
Group 2	13.7 ± 1.1	13.8 ± 0.8	13.4 ± 0.8

Values are mean ± SD. As expected, Pa<sub>CO<sub>2</sub></sub> and pH values in hypercapnia are significantly different ( $P < 0.01$ ) from normocapnia.

\*  $P < 0.05$  versus group 1.

†  $P < 0.01$  versus group 1.

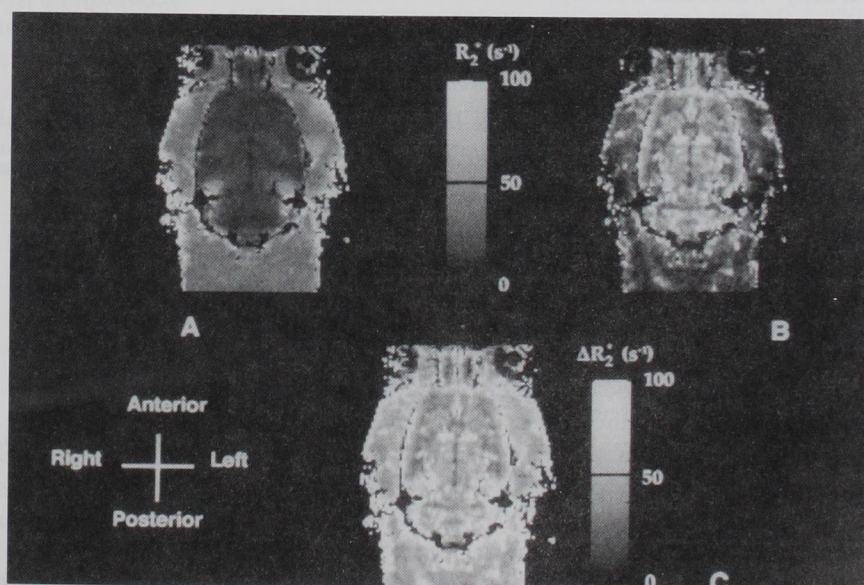
## Results

Table 1 shows physiologic and biochemical data for groups 1 and 2. No significant changes in mean arterial blood pressure, temperature, PaO<sub>2</sub>, and hemoglobin values were found during the successive periods. Despite

comparable procedures, differences in PaO<sub>2</sub> and in temperature values were found between the two groups (table 1). Figures 1A and B show typical R<sub>2</sub>\* images of the coronal section before and after injection of the contrast agent, respectively, during normocapnia. Administration of the contrast agent results in an increase in R<sub>2</sub>\* values, leading to positive ΔR<sub>2</sub>\* in the cerebral regions (fig. 1C).

Values of ΔR<sub>2</sub>\* in cerebral and extracerebral regions are shown in table 2 (group 1) and in table 3 (group 2) throughout the successive Pa<sub>CO<sub>2</sub></sub> periods. In both groups, ΔR<sub>2</sub>\* (*i.e.*, CPV) was less in extracerebral tissue and in striatum than in neocortex and in cerebellum during normocapnia. In group 2, unilateral carotid ligation did not result in significant interhemispheric differences in CPV in the striatum and in the neocortex during normocapnia. Hypercapnia resulted in a statistically significant CPV increase in striatum, neocortex and cerebellum compared with the normocapnic control values in group 1 and in group 2 ( $P < 0.01$ ). Surprisingly, the left side of the neocortex had higher CPV values than the right side in group 1. Left carotid occlusion led to a significantly reduced CPV response to hypercapnia in the ipsilateral side of the striatum and neocortex compared with the unclamped side in group 2 (table 3 and fig. 2). In both groups of rats, the CPV changes were reversed by the carbon dioxide washout period. There was no statistically significant CPV change in the extracerebral tissue regardless of the Pa<sub>CO<sub>2</sub></sub> periods in groups 1 and 2.

Table 4 shows regional increases in CPV during hyper-



**Fig. 1.** Typical coronal R<sub>2</sub>\* images (5 mm below bregma) before (A) and after (B) the injection of contrast agent (AMI-227; 200 μmol iron per kilogram of body mass). T<sub>R</sub> = 1.5 s; slice thickness = 1 mm; field of view = 4 cm; 64×64 image matrix; number of accumulation = 2; number of echoes = 8. In C, the ΔR<sub>2</sub>\* map was derived from removal of A to the B image. The lightest points correspond to the highest CPV values.



**Table 2.  $\Delta R_2^*$  Values ( $s^{-1}$ ) in Group 1 (No Carotid Occlusion) throughout the Successive  $Pa_{CO_2}$  Periods**

	Normocapnia	Hypercapnia	Recovery
Striatum			
Right side	42.0 $\pm$ 6.2	59.7 $\pm$ 6.5*	41.5 $\pm$ 5.8
Left side	41.9 $\pm$ 5.2	58.6 $\pm$ 6.6*	41.2 $\pm$ 4.6
Neocortex			
Right side	59.9 $\pm$ 4.5	79.1 $\pm$ 4.8*	63.0 $\pm$ 5.6
Left side	60.1 $\pm$ 4.3	81.9 $\pm$ 5.6*†	60.9 $\pm$ 3.3
Cerebellum	51.4 $\pm$ 4.1	76.2 $\pm$ 5.8*	50.0 $\pm$ 4.3
Extracerebral tissue	32.3 $\pm$ 4.2	31.7 $\pm$ 4.5	31.3 $\pm$ 4.3

Values are mean  $\pm$  SD.

\*  $P < 0.01$  versus normocapnia.

†  $P < 0.05$  versus right side.

capnia in groups 1 and 2. The left striatum of group 2 (clamped side) had significantly lower CPV response to carbon dioxide than did that of group 1. No difference between the two groups was found regarding the CPV response of the cerebellum and of the extracerebral tissue.

In group 3 (no contrast agent, left carotid ligation),  $R_2^*$  ( $=1/T_2^*$ ) was measured during normocapnia ( $Pa_{CO_2} = 34 \pm 1.7$  mmHg) and hypercapnia ( $Pa_{CO_2} = 59 \pm 16.8$  mmHg). The  $R_2^*$  values in the striatum, neocortex, and cerebellum were significantly less during hypercapnia compared with normocapnia, leading to negative absolute  $\Delta R_2^*$  values in these regions ( $-0.6 \pm 0.7$ ,  $-2.1 \pm 1.0$ , and  $-0.8 \pm 0.5 s^{-1}$ , respectively;  $P < 0.05$ ). No significant difference in striatal and neocortical  $\Delta R_2^*$  was found between the two hemispheres. The change in  $R_2^*$  in the extracerebral tissue ( $\Delta R_2^* = -0.2 \pm 1.6 s^{-1}$ ) was not statistically significant.

## Discussion

There are two main approaches to determine CPV (or CBV if a constant cerebral hematocrit is assumed) using contrast-enhanced MRI. In the dynamic susceptibility-contrast MRI approach, a bolus of an intravascular paramagnetic contrast agent was shown to change the NMR signal as it passed through the vascular bed.<sup>16</sup> The bolus produces transient local magnetic field inhomogeneities, leading to a reduction in  $T_2^*$  of the bulk tissue. Relative CBV maps have been obtained from the area under the  $\Delta R_2^*$  curve during the first bolus passage in human gray and white matter.<sup>17</sup> The CBV changes of a large section of the middle cerebral artery territory were recently assessed in patients with occlusive cerebrovas-

cular disease during acetazolamide administration.<sup>18</sup> However, repeated CBV measurements for cerebrovascular reactivity testing require a time interval depending on the clearance of the contrast agent from the plasma. Furthermore, the signal-to-noise ratio and the spatial resolution of these NMR images are reduced by the short time allowed for image acquisition. Conversely, relative changes in CBV can be determined by the steady state susceptibility-contrast MRI approach. This approach has been used successfully to monitor CBV changes during various stimulations.<sup>19-23</sup> The study of Jones *et al.*<sup>23</sup> done during 60 s of anoxia in rat brain and our study are the first reports of intrahemispheric measurements of CBV changes. In addition, our results show that the effects of carotid occlusion on the CPV changes induced by moderate reversible hypercapnia can be measured in the ipsilateral hemisphere of a rat brain, indicating the high sensitivity of this method to detect a decrease in the cerebrovascular reserve capacity.

The ability of the ultrasmall superparamagnetic iron oxide agents (*e.g.*, AMI-227) to enhance magnetic resonance contrast has been described.<sup>24</sup> As these are not initially recognized by the reticuloendothelial system because of their small hydrodynamic diameter and the hydrophilic dextran coating,<sup>22</sup> the plasma elimination half-time of such agents is prolonged. Contrast-enhanced MRI thus can be performed *via* a steady-state approach. Boxerman *et al.*<sup>12</sup> found good agreement between the predictions of CBV based on a Monte Carlo model and the experimental data obtained from the serial injection of AMI-227 used as a blood pool contrast agent. This contrast agent has been used to monitor hyperemia in a feline model of transient global isch-

**Table 3.  $\Delta R_2^*$  Values ( $s^{-1}$ ) in Group 2 (Left Carotid Occlusion) throughout the Successive  $Pa_{CO_2}$  Periods**

	Normocapnia	Hypercapnia	Recovery
Striatum			
Right side	37.6 $\pm$ 4.6	49.7 $\pm$ 2.9*	33.5 $\pm$ 4.7
Left side	36.9 $\pm$ 4.8	44.8 $\pm$ 3.2*†	33.5 $\pm$ 5.0
Neocortex			
Right side	55.8 $\pm$ 5.3	76.4 $\pm$ 6.5*	52.3 $\pm$ 5.6
Left side	54.9 $\pm$ 6.6	69.5 $\pm$ 10.0*†	51.0 $\pm$ 10.0
Cerebellum	54.0 $\pm$ 6.4	78.8 $\pm$ 6.5*	54.8 $\pm$ 8.2
Extracerebral tissue	27.3 $\pm$ 9.1	26.8 $\pm$ 9.6	27.4 $\pm$ 9.4

Values are mean  $\pm$  SD.

\*  $P < 0.01$  versus normocapnia.

†  $P < 0.05$  versus right side.

‡  $P < 0.01$  versus right side.



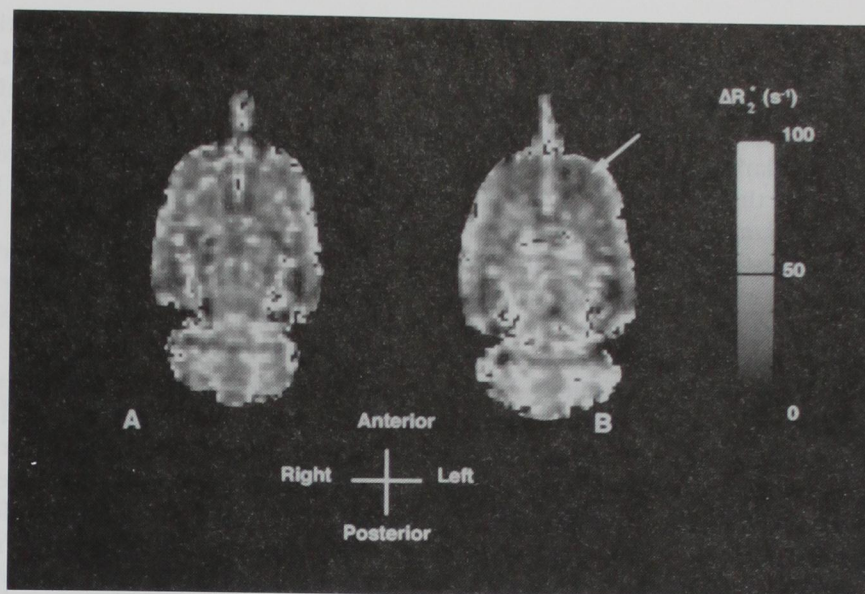
CO<sub>2</sub>-INDUCED REGIONAL CHANGES IN CEREBRAL PLASMA VOLUME

Fig. 2. Typical cerebral  $\Delta R_2^*$  maps (5 mm below bregma) during hypercapnia in a normal rat (A) and in a rat with a left carotid occlusion (B).  $T_R = 1.5$  s; slice thickness = 1 mm; field of view = 4 cm;  $64 \times 64$  image matrix; number of accumulations = 2; number of echoes = 8. The extracerebral tissue has been removed from the images. The left carotid ligation decreases the ipsilateral striatal CPV response to carbon dioxide, as reflected by smaller  $\Delta R_2^*$  values (arrow) compared with those in the unclamped side.

emia<sup>21</sup> and to enhance the signal changes induced by apnea in the rabbit,<sup>22</sup> and it is undergoing further investigation in clinical trials. However, the approach we report here is valid under certain conditions, as previously noted by Hamberg *et al.*<sup>21</sup> First, the plasma concentration of the contrast agent must be unchanged during the 3-min acquisition time of the NMR images. This was reasonably the case considering the elimination half-time of this agent. Although there remains uncertainty about the exact correction factor for the clearance of agent, the plasma clearance was probably minimal in this study because the postcontrast experiment

lasted 60 min. Second, the contrast agent must be confined to the intravascular compartment. In the case of blood-brain barrier disruption, the carbon dioxide-induced changes in CPV could be underestimated because of the decreased susceptibility difference between vessels and tissue. However, a breakdown of the blood-brain barrier is unlikely with our model because reversible  $\Delta R_2^*$  changes were observed during the carbon dioxide washout period. Third, CPV measurements and correction for plasma clearance of contrast agents were based on the assumed linear relation between CPV (or contrast agent plasma concentration) and  $\Delta R_2^*$ . This assumption was verified in previous studies.<sup>12,13</sup>

The plasma concentration of the contrast agent must be large enough so that the steady state susceptibility difference between vascular and extravascular compartments is much larger than susceptibility changes of the blood. Indeed, hypercapnia increases CBF without significantly altering rates of cerebral metabolism. Thus the blood concentration of the paramagnetic deoxyhemoglobin is expected to decrease, leading to a change in the  $T_2^*$  of blood. The resulting decrease in  $R_2^*$  could be compensated partly by an increase in  $R_2^*$  due to the hypercapnia-induced CBV changes. This mechanism could explain the lower  $R_2^*$  values observed during hypercapnia compared with normocapnia in group 3, which corresponds to findings of other studies in which no contrast agent was administered.<sup>25,26</sup> However, the magnitude of the deoxyhemoglobin-induced  $\Delta R_2^*$  is small (<10% of normo-

Table 4. Regional CPV Response to Hypercapnia (% Value in Normocapnia  $\times 100$ ) in Group 1 (No Carotid Occlusion) and Group 2 (Left Carotid Occlusion)

	Group 1	Group 2
Striatum		
Right side	143 $\pm$ 7	134 $\pm$ 15
Left side	140 $\pm$ 9	123 $\pm$ 14†‡
Neocortex		
Right side	132 $\pm$ 6	138 $\pm$ 16
Left side	136 $\pm$ 6*	127 $\pm$ 17*
Cerebellum	149 $\pm$ 12	147 $\pm$ 15
Extracerebral tissue	98 $\pm$ 4	98 $\pm$ 7

Values are mean  $\pm$  SD.

\*  $P < 0.05$  versus right side.

†  $P < 0.01$  versus right side.

‡  $P < 0.01$  versus group 1.



capnic values<sup>25,26</sup>;  $0.5\text{--}2\text{ s}^{-1}$  in the present study) compared with that observed in the presence of a contrast agent (see tables 2 and 3). This explains why no abnormal cerebrovascular reactivity was detected in group 3.

The relation between  $\Delta R_2^*$  and CPV should not depend on the pulse sequence or on the distribution of vessel diameters. It was shown recently that use of spin-echo imaging techniques allow the responsiveness of the microvascular bed to be measured selectively.<sup>12</sup> Conversely, the authors found that  $\Delta R_2^*$  changes can be detected at all vessel radii, reaching a plateau for vessel radius  $>10\text{ }\mu\text{m}$  using a gradient-echo pulse sequence. Furthermore, this  $\Delta R_2^*$  plateau should be reached for capillaries when a high dose of contrast agent is used, as occurred in the present study, resulting in a large intra-extravascular susceptibility difference.<sup>13</sup> Therefore, the dose of contrast agent, and the gradient-echo pulse sequence we used here, were adequate to detect vascular volume changes within brain parenchyma. This method allowed us to observe differences between cerebral regions during normocapnia, because the CPV in the neocortex and in the cerebellum were 1.2–1.5 times higher than that of the striatum in groups 1 and 2. These results are similar to those found in awake normocapnic rats using autoradiography.<sup>5,9,10</sup>

Using this method, we detected CPV changes only. Extrapolation to CBV should assume that the cerebral hematocrit value remains constant during the experiment. However, separated measurements of both cerebral erythrocyte volume and CPV have shown that the increase in CPV is larger than for cerebral erythrocyte volume in humans<sup>8</sup> and rats<sup>5,6</sup> during hypercapnia. No measurement of the CBV response to carbon dioxide thus can be made using contrast-enhanced MRI. We found that moderate hypercapnia significantly increased the CPV in the absence of any significant changes in arterial blood pressure. The reversible effect on CPV during carbon dioxide washout and the expected absence of any changes in extracerebral signal intensities with varying  $\text{Pa}_{\text{CO}_2}$  argue for the sensitivity of this method as a noninvasive monitor of the response of intracerebral plasma volume to carbon dioxide.

*In vivo* determination of the CBV response to carbon dioxide (expressed as a percentage change per millimeter of mercury of  $\text{Pa}_{\text{CO}_2}$ ) showed comparable values, ranging from 0.9 to 1.2 %/mmHg  $\text{Pa}_{\text{CO}_2}$  in humans,<sup>7</sup> primates,<sup>3</sup> goats,<sup>27</sup> and rats,<sup>4</sup> although Sakai *et al.*<sup>8</sup> found higher values in humans (2.2 %/mmHg

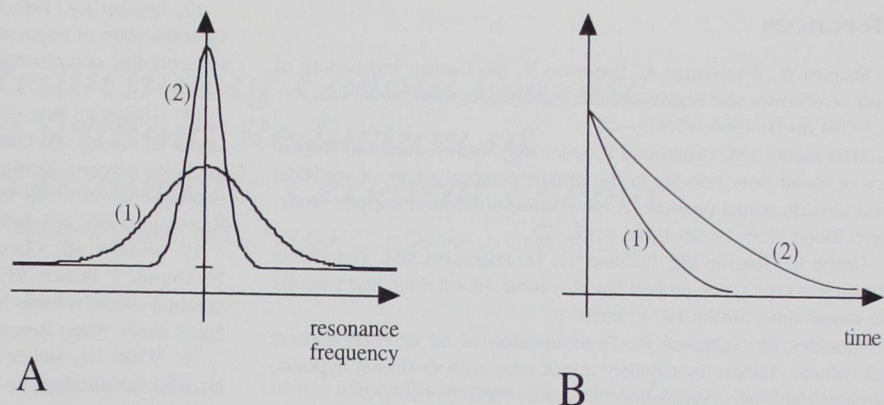
$\text{Pa}_{\text{CO}_2}$ ). From these data, an increase in CBV of 30–35% is expected when  $\text{Pa}_{\text{CO}_2}$  increases by approximately 30 mmHg, a result that corresponds with our 35–50% CPV changes in group 1. However, recent studies reported only a 10–25% CPV change in rats during severe hypercapnia.<sup>5,6</sup> Different explanations could account for these discrepancies. First, our protocol was performed during anesthesia with halothane, which results in a 12% increase in CBV in normocapnic dogs.<sup>28</sup> Previous studies were, however, performed in anesthetized animals without the use of a volatile agent.<sup>3,4,27</sup> Second, in the studies of Bereczki *et al.*<sup>5</sup> and Keyeux *et al.*,<sup>6</sup> CPV was determined by autoradiography in animals killed by decapitation, which may decrease the measured CBV (and CPV) because of the possible loss of radiolabeled blood during brain removal.<sup>29</sup> Third, Bereczki *et al.*<sup>5</sup> assessed the CPV in microvessels with luminal radii  $<25\text{ }\mu\text{m}$ . Our method, used during moderate hypercapnia, includes the volume present in vessels of various sizes, probably larger intraparenchymal vessels. However, the inclusion of the pial vasculature remains unlikely in the selected coronal images.

Unilateral carotid ligation significantly reduces the CPV response to hypercapnia in the striatum and neocortex in the ipsilateral side of the occlusion (group 2). In addition, comparison of groups 1 and 2 suggests that the striatum is more sensitive to carotid ligation than are the other cerebral regions. The higher  $\text{Pa}_{\text{O}_2}$  values in group 1 compared with group 2 (see table 1) would attenuate in part the signal intensity changes during hypercapnia in this group, as shown by Berry *et al.*<sup>22</sup> Knowing the effects of body temperature on cerebral vasculature, similar effects on NMR signal would be expected in group 1 where rectal temperature was slightly less than that in group 2. Despite experimental conditions *a priori* that were less favorable in group 1 than in group 2, we must be cautious when comparing the two groups because no determination of CPV was performed before the carotid ligation in group 2. It has been shown that this occlusion results in a CBF reduction of approximately 20% in the area confined to the middle cerebral artery region in the ligated side during control conditions.<sup>30</sup> Conversely, the CBF response to hypercapnia is markedly asymmetrical because the increase in CBF in the ipsilateral side is only 50% of that in the unclamped side.<sup>14</sup> The metabolic response to hypoxic hypoxia is also strongly impaired in the ipsilateral neocortical side.<sup>31</sup> Our findings indicate that carotid occlusion also af-



CO<sub>2</sub>-INDUCED REGIONAL CHANGES IN CEREBRAL PLASMA VOLUME

Fig. 3. Schematic representation of the distribution of resonance frequencies (A) and evolution of the free induction decay (B) in a voxel, in the presence (1) and in the absence (2) of a contrast agent.



fects the ipsilateral CPV response to hypercapnia. Because the CBF<sup>14</sup> and the CPV are, however, increased during hypercapnia even in the ligated side, these results show that the ipsilateral cerebrovascular reserve capacity has been decreased. Furthermore, the more important reduction in the CPV response to carbon dioxide in the striatum compared with that in the neocortex reflects the distribution territory of such a ligation. No reduction in CPV of the cerebellum was noted, as expected in this model in which the posterior circulation remains unaffected.<sup>30</sup>

In conclusion, a contrast-enhanced MRI method was used to detect noninvasively changes in CPV during moderate variations in PaCO<sub>2</sub> within various brain regions in anesthetized rats. Regional differences in the CPV between striatum, neocortex, and cerebellum in normocapnia and the CPV changes induced by hypercapnia within these brain regions are in accordance with the results obtained with other methods. Furthermore, the ipsilateral decrease in the cerebrovascular reserve capacity induced by unilateral carotid ligation was detected. These results show that regional CPV changes can be assessed in the rat brain *in vivo*. This form of MRI reactivity testing might be useful for designing diagnostic testing in humans.

## Appendix

The magnetic field in a sample ( $\vec{B}$ ) depends both on the strength of the magnet and on the materials that comprise the sample, as described by the formula:

$$\vec{B} = \vec{B}_0(1 + \chi) \quad (5)$$

where  $\chi$  is the magnetic susceptibility constant of the sample and

$\vec{B}_0$  the magnetic field in the absence of sample. In tissue,  $\chi$  is very small and negative (the magnetic field  $B$  in the tissue is smaller than  $B_0$ ). Such substances are called diamagnetic ( $\chi = -10^{-5}$  to  $-10^{-6}$ ). In some materials,  $\chi$  is positive and they are called paramagnetic or superparamagnetic. In the latter case,  $\chi$  depends on the magnetic field strength. Paramagnetic materials (such as deoxyhemoglobin, oxygen, and nitric oxide) have positive  $\chi$  values ( $\chi = 10^{-3}$  to  $10^{-5}$ ). Magnetic resonance imaging contrast agents are either paramagnetic (e.g., gadolinium-DPTA) or superparamagnetic (e.g., AMI-227).

The presence of an MRI contrast agent in the blood pool induces a susceptibility difference ( $\Delta\chi$ ) between vascular and extravascular compartments, which is proportional to the concentration of the contrast agent. Due to this susceptibility difference, the magnetic field around the vessels is not homogeneous (fig. 3A). Thereby the resonance frequency, which is proportional to the magnetic field, varies through the voxel.

The NMR signal  $S(t)$  created by a radiofrequency pulse decays with a time constant  $T_2^*$ , according to the formula:

$$S(t) = S_0 \exp - t/T_2^* \quad (6)$$

where  $S_0$  is the signal intensity immediately after the radiofrequency pulse. The presence of macroscopic and microscopic magnetic field inhomogeneities creates a distribution of resonance frequencies that increases the signal decay rate. Thus the presence of a contrast agent in the blood pool results in a decrease in  $T_2^*$  (fig. 3B) or equivalently in an increase in relaxation rate  $R_2^*$ , where  $R_2^* = 1/T_2^*$ .

The changes in  $R_2^*$  ( $\Delta R_2^*$ ) due to the injection of a contrast agent are mainly due to the dephasing of the extravascular spins in the spatially nonuniform field created by the magnetic susceptibility difference between vascular and extravascular compartments. The value of  $\Delta R_2^*$  has been shown to be linearly proportional to the mean concentration of the contrast agent in the volume of interest (i.e., to the product of its blood concentration by CBV).<sup>12,13</sup> The relaxation rates  $R_2^*$ , and thus their changes  $\Delta R_2^*$ , can be determined with gradient echo techniques that are sensitive to macro- and microvasculature.<sup>12</sup>

The authors thank Jean-Luc Bosson and Dan Veale for helpful comments on the study.



## References

1. Shapiro W, Wasserman AJ, Patterson JL: Mechanism and pattern of human cerebrovascular regulation after rapid changes in blood CO<sub>2</sub> tension. *J Clin Invest* 1966; 45:913-22
2. Markwalder TM, Grolimund P, Seiler RW, Roth F, Aaslid R: Dependency of blood flow velocity in the middle cerebral artery on end-tidal carbon dioxide partial pressure. A transcranial ultrasound doppler study. *J Cereb Blood Flow Metab* 1984; 4:368-72
3. Grubb RL, Raichle ME, Eichling JO, Ter-Pogossian MM: The effects of changes in PaCO<sub>2</sub> on cerebral blood volume, blood flow, and vascular mean transit time. *Stroke* 1974; 5:630-9
4. Shockley RP, LaManna JC: Determination of rat cerebral cortical blood volume changes by capillary transit time analysis during hypoxia, hypercapnia and hyperventilation. *Brain Res* 1988; 454:170-8
5. Bereczki D, Wei L, Otsuka T, Hans FJ, Acuff V, Patlak C, Fenstermacher J: Hypercapnia slightly raises blood volume and sizably elevates flow velocity in brain microvessels. *Am J Physiol* 1993; 264:H1360-9
6. Keyeux A, Ochrymowicz-Bemelmans D, Charlier AA: Induced response to hypercapnia in the two-compartment total cerebral blood volume: influence on brain vascular reserve and flow efficiency. *J Cereb Blood Flow Metab* 1995; 15:1121-31
7. Greenberg JH, Alavi A, Reivich M, Kuhl D, Uzzell B: Local cerebral blood volume response to carbone dioxide in man. *Circ Res* 1978; 43:324-31
8. Sakai F, Nakazawa K, Tazaki Y, Ishii K, Hino H, Igarashi H, Kanda T: Regional cerebral blood volume and hematocrit measured in normal human volunteers by single-photon emission computed tomography. *J Cereb Blood Flow Metab* 1985; 5:207-13
9. Cremer JE, Seville MP: Regional brain blood flow, blood volume, and haematocrit values in the adult rat. *J Cereb Blood Flow Metab* 1983; 3:254-6
10. Tajima A, Nakata H, Lin SZ, Acuff V, Fenstermacher J: Differences and similarities in albumin and red blood cell flows through cerebral microvessels. *Am J Physiol* 1992; 262:H1515-24
11. Rosen BR, Belliveau JW, Vevea JM, Brady TJ: Perfusion imaging with NMR contrast agents. *Magn Reson Med* 1990; 14:249-65
12. Boxerman JL, Hamberg LM, Rosen BR, Weisskoff RM: MR contrast due to intravascular magnetic susceptibility perturbations. *Magn Reson Med* 1995; 34:555-66
13. Fisel CR, Ackerman JL, Buxton RB, Garrido L, Belliveau JW, Rosen BR, Brady TJ: MR contrast due to microscopically heterogeneous magnetic susceptibility: Numerical simulations and applications to cerebral physiology. *Magn Reson Med* 1991; 17:336-47
14. De Ley G, Nshimyumuremyi JB, Leusen I: Hemispheric blood flow in the rat after unilateral common carotid occlusion: Evolution with time. *Stroke* 1985; 16:69-73
15. Paxinos G, Watson C: *The Rat Brain in Stereotaxic Coordinates*. North Ryde, Academic Press Australia, 1982
16. Belliveau JW, Rosen BR, Kantor HL, Rzedzian RR, Kennedy DN, McKinstry RC, Vevea JM, Cohen MS, Pykett IL, Brady TJ: Functional cerebral imaging by susceptibility-contrast NMR. *Magn Reson Med* 1990; 14:538-46
17. Rempp KA, Brix G, Wenz F, Becker CR, Gückel F, Lorenz WJ: Quantification of regional cerebral blood flow and volume with dynamic susceptibility contrast-enhanced MR imaging. *Radiology* 1994; 193:637-41
18. Gückel FJ, Brix G, Schmiedek P, Piepgras A, Becker G, Köpke J, Gross H, Georgi M: Cerebrovascular reserve capacity in patients with occlusive cerebrovascular disease: assessment with dynamic susceptibility contrast-enhanced MR imaging and the acetazolamide stimulation test. *Radiology* 1996; 201:405-12
19. Moseley ME, Chew WM, White DL, Kucharczyk J, Litt L, Derugin N, Dupon J, Brasch RC, Norman D: Hypercarbia-induced changes in cerebral blood volume in the cat: A <sup>1</sup>H MRI and intravascular contrast agent study. *Magn Reson Med* 1992; 23:21-30
20. White DL, Aicher KP, Tzika AA, Kucharczyk J, Engelstad BL, Moseley ME: Iron-dextran as a magnetic susceptibility contrast agent: Flow-related contrast effects in the T2-weighted spin-echo MRI of normal rat and cat brain. *Magn Reson Med* 1992; 24:14-28
21. Hamberg LM, Boccalini P, Stranjalis G, Hunter GJ, Huang Z, Halpern E, Weisskoff RM, Moskowitz MA, Rosen BR: Continuous assessment of relative cerebral blood volume in transient ischemia using steady state susceptibility-contrast MRI. *Magn Reson Med* 1996; 35:168-73
22. Berry I, Benderbous S, Ranjeva JP, Gracia-Meavilla D, Manelfe C, Le Bihan D: Contribution of Sinerem<sup>®</sup> used as blood-pool contrast agent: Detection of cerebral blood volume changes during apnea in the rabbit. *Magn Reson Med* 1996; 36:415-9
23. Jones RA, Haraldseth O, Baptista AM, Müller TB, Øksendal AN: A study of the contribution of changes in the cerebral blood volume to the haemodynamic response to anoxia in rat brain. *NMR Biomed* 1996; 9:233-40
24. Chambon C, Clement O, Le Blanche A, Schouman-Claeys E, Frija G: Superparamagnetic iron oxides as positive MR contrast agents: in vitro and in vivo evidence. *Magn Res Imaging* 1993; 11:509-19
25. Graham GD, Zhong J, Petroff OAC, Constable RT, Prichard JW, Gore JC: BOLD MRI monitoring of changes in cerebral perfusion induced by acetazolamide and hypercarbia in the rat. *Magn Reson Med* 1994; 31:557-60
26. Rostrup E, Larsson HBW, Toft PB, Garde K, Thomsen C, Ring P, Søndergaard L, Henriksen O: Functional MRI of CO<sub>2</sub> induced increase in cerebral perfusion. *NMR Biomed* 1994; 7:29-34
27. Smith AL, Neufeld GR, Ominsky AJ, Wollman H: Effect of arterial CO<sub>2</sub> tension on cerebral blood flow, mean transit time, and vascular volume. *J Appl Physiol* 1971; 31:701-7
28. Artru AA: Relationship between cerebral blood volume and CSF pressure during anesthesia with halothane or enflurane in dogs. *ANESTHESIOLOGY* 1983; 58:533-9
29. Todd MM, Weeks JB, Warner DS: Microwave fixation for the determination of cerebral blood volume in rats. *J Cereb Blood Flow Metab* 1993; 13:328-36
30. Salford LG, Siesjö BK: The influence of arterial hypoxia and unilateral carotid artery occlusion upon regional blood flow and metabolism in the rat brain. *Acta Physiol Scand* 1974; 92:130-41
31. Payen JF, LeBars E, Wuyam B, Tropini B, Pépin JL, Lévy P, Décorps M: Lactate accumulation during moderate hypoxic hypoxia in neocortical rat brain. *J Cereb Blood Flow Metab* 1996; 16:1345-52